

东昆仑百吨沟花岗岩岩石地球化学、锆石 U-Pb 年龄 与 Hf 同位素特征及其构造意义

韩 玉^{1,2,3}, 王启林⁴, 谢海林³, 陈苏龙³, 李少南³, 李玉莲³, 王 斌³,
张政治³, 王 雷³, 马志全³, 郭 伟³

(1. 中国科学院大学, 北京 100049; 2. 中国科学院 青藏高原研究所, 北京 100101; 3. 青海省第一地质勘查院,
青海 平安 810600; 4. 中国地质大学 资源学院, 湖北 武汉 430074)

摘要: 东昆仑造山带志留纪-泥盆纪的演化存在着争议, A型花岗岩常用来限定造山过程中构造转换的时间。百吨沟花岗岩岩体位于东昆仑造山带东段的五龙沟金矿集区, 目前缺乏系统的研究, 本文对其进行了岩石地球化学、锆石 U-Pb 年代学及 Hf 同位素研究。锆石 U-Pb 定年表明, 该岩体结晶年龄为 417.9 ± 3.5 Ma。岩石地球化学分析结果显示, 岩石高硅 ($\text{SiO}_2 = 71.2\% \sim 77.2\%$)、富碱 ($\text{K}_2\text{O} + \text{Na}_2\text{O} = 8.23\% \sim 10.70\%$)、低 MgO ($0.04\% \sim 0.22\%$) 和 CaO ($0.09\% \sim 0.95\%$), 具有富集大离子亲石元素 (Rb, K, Th, U)、亏损高场强元素 (P, Ti) 的特征, 具有明显的负铕异常和“海鸥型”稀土元素配分模式, 并且岩石具有较高的 Ga/Al 、 TiFeO/MgO 值以及 Zr 饱和温度, 表明该岩体为 A型花岗岩。此外, 锆石的 $\varepsilon\text{Hf}(t) = -0.6 \sim 1.9$, 对应的二阶段模式年龄 t_{2DM} 介于 1442~1284 Ma 之间, 推测该 A型花岗岩主要源自早期具有相似 Hf 同位素的长英质火成岩部分熔融。该花岗岩具有 A2型花岗岩的特征, 指示其形成于后碰撞伸展环境。东昆仑造山带发育大量近同时的 A2型花岗岩, 反映其在晚志留世时进入后碰撞伸展阶段。

关键词: A型花岗岩; 岩石地球化学; 后碰撞伸展; 五龙沟; 东昆仑造山带

中图分类号: P588.12⁺1; P597

文献标识码: A

文章编号: 1000-6524(2024)06-1448-17

Geochemistry, zircon U-Pb chronology and Hf isotopes of the Baidungou granite from the East Kunlun Orogen and their implications

HAN Yu^{1,2,3}, WANG Qi-lin⁴, XIE Hai-lin³, CHEN Su-long³, LI Shao-nan³, LI Yu-lian³,
WANG Bin³, ZHANG Zheng-zhi³, WANG Lei³, MA Zhi-quan³ and GUO Wei³

(1. University of Chinese Academy of Sciences, Beijing 100049, China; 2. Institute of Tibetan Plateau Research, Chinese Academy of Sciences, Beijing 100101, China; 3. Qinghai No. 1 Academy of Geology and Mineral Exploration, Ping'an 810600, China;
4. School of Earth Resources, China University of Geosciences, Wuhan 430074, China)

Abstract: The Silurian-Devonian evolution of the East Kunlun Orogen (EKO) is controversial. A-type granites are often used to constrain the timing of tectonic transformation during the orogenic process. The Baidungou granite pluton, located in the Wulonggou goldfield in the eastern part of the EKO, has not been systematically studied in previous research. Therefore, this paper takes it as the research object to study its petrogeochemistry, zircon U-Pb geochronology and Hf isotopes. The zircon U-Pb dating shows the crystallization age of the intrusion is 417.9 ± 3.5 Ma. Petrogeochemical studies reveal that the intrusion is characterized by high silicon ($\text{SiO}_2 = 71.2\% \sim 77.2\%$)

收稿日期: 2024-05-18; 接受日期: 2024-10-14; 编辑: 郝艳丽

基金项目: 青海省人才办、青海省地质矿产勘查开发局及青海省第一地质勘查院联合资助项目(青地矿科[2017]7号)

作者简介: 韩 玉(1985-), 男, 博士研究生, 高级工程师, 从事地质矿产勘查及矿床学研究, E-mail: hanyu@itpcas.ac.cn; 通讯作者:
王启林(1995-), 男, 博士研究生, 矿产普查与勘探专业, E-mail: wangqilin@cug.edu.cn。

and alkali ($K_2O+Na_2O=8.23\% \sim 10.7\%$), low MgO ($0.04\% \sim 0.22\%$) and CaO ($0.09\% \sim 0.95\%$), enriched large ion lithophile elements (Rb, K, Th, U), depleted high field strength elements (P, Ti), obvious negative europium anomaly, and ‘gull type’ REE patterns. Combined with high Ga/Al and $TFeO/MgO$ values and Zr saturation temperatures of whole rocks, the intrusion is classified as A-type granite. In addition, the zircon $\varepsilon Hf(t)$ values vary from -0.6 to 1.9 and two-stage Hf model ages range from $1\,442$ to $1\,284$ Ma, suggesting that this A-type granite was mainly derived from the partial melting of early felsic magmatic rocks with similar Hf isotopes. This granite exhibits characteristics of the A2-type, indicating that it formed in a post-orogenic extensional environment. The EKO developed a large number of A2-type granites nearly contemporaneous with this granite, reflecting it had entered the post-collision extension stage during the Late Silurian.

Key words: A-type granite; petrogeochemistry; post-collisional extension; Wulonggou; East Kunlun Orogen

Fund support: The Joint Funding Project by the Talent Office, the Bureau of Geological Exploration and Development (BGED), and No. 1 Academy of Geology and Mineral Exploration of Qinghai Province (Geological Technology Office of the BGED of Qinghai Province [2017] No. 7)

东昆仑造山带位于青藏高原北缘,是中央造山带重要的组成部分(陆松年等,2006;许志琴等,2006)。该造山带处于原特提斯洋向古特提斯洋转变的关键位置(Dong *et al.*, 2021; Fu *et al.*, 2022),记录了大量与原特提斯洋和古特提斯洋演化有关的构造-岩浆活动(Dong *et al.*, 2018)。与俯冲相关的蛇绿岩最早出现在约 520 Ma,指示原特提斯洋在寒武纪时已经开始俯冲(Fu *et al.*, 2022),然而之后原特提斯洋在东昆仑的演化存在着争议。一种观点认为俯冲作用持续到早泥盆世,比如Duan等(2020)认为岩浆源区从黑山玄武岩(445 Ma)的亏损地幔向夏日哈木辉长岩(427 Ma)的富集地幔变化与俯冲有关,Li等(2015)认为夏日哈木的超基性岩(412 Ma)来源于俯冲相关的玻安岩;另一种观点认为原特提斯洋在志留纪-早泥盆世经历碰撞造山过程,A型花岗岩(Chen *et al.*, 2020; Zhang *et al.*, 2021)和磨拉石沉积(陆露等,2010)的出现与后碰撞的伸展有关。

A型花岗岩对伸展环境具有良好的指示意义,常用来限定造山过程中构造转换的时间(吴福元等,2007;吴锁平等,2007;贾小辉等,2009;张旗等,2012)。东昆仑造山带加里东期A型花岗岩零星出露但分布较广,西起阿尔金断裂带南侧白干湖地区($422 \sim 414$ Ma)(李国臣等,2012; Zhou *et al.*, 2016),东至阿尼玛卿蛇绿岩带北侧呼德生地区(413 ± 2.3 Ma)(曹锦山等,2023)。东昆仑东段(格尔木以东)五龙沟地区A型花岗岩的报道主要集中在矿区中部,也即是水闸西沟至红旗沟一带(王艺龙等,2018; Xin *et al.*, 2018; Ding *et al.*, 2019; Chen

et al., 2020),年龄跨度从 427 Ma(Zhang *et al.*, 2021)到 390 Ma(胡继春等,2017)。最近的研究发现萤石沟北侧的花岗闪长岩为I型(403 Ma, Zhang *et al.*, 2021),最新的地质调查发现百吨沟岩体尖灭于红石岭和红旗沟南部,目前缺乏系统研究。因此,本文对百吨沟岩体进行岩石地球化学、锆石年代学和Hf同位素的研究,确定其侵位时间,探讨其岩石成因和构造环境,以期为东昆仑造山带原特提斯洋的演化提供新的参考。

1 区域地质背景

东昆仑造山带作为中央造山带的一部分,西起于阿尔金断裂带,东接西秦岭,北为柴达木盆地,南为巴颜喀拉-松潘甘孜地体,其自北向南可分为昆北带、昆中带和昆南带(图1),分别以3条近东西向的深大断裂相隔。昆北带出露的地层主要是奥陶纪祁漫塔格群,岩浆作用以华力西期(晚古生代)二长花岗岩和花岗闪长岩为主(高永宝,2013);昆中带出露大量以华力西期和印支期为主的花岗岩,地层则以前寒武纪金水口群与冰沟群为主(高永宝,2013; Yan *et al.*, 2019),其东段分布着少量加里东期的榴辉岩(国显正等,2018);昆南带是大量三叠系的复理石沉积不整合于元古界苦海群或万宝沟群之上(王国灿等,2007),零星见早古生代-中生代花岗岩的侵入体(Dong *et al.*, 2018; Zhao *et al.*, 2019)。沿着3条深大断裂带都有蛇绿岩套的出露,其中,昆北断裂带主要在西段(格尔木以西)出现志留纪的蛇绿岩残块,昆中断裂带在其东段出现寒武纪、志

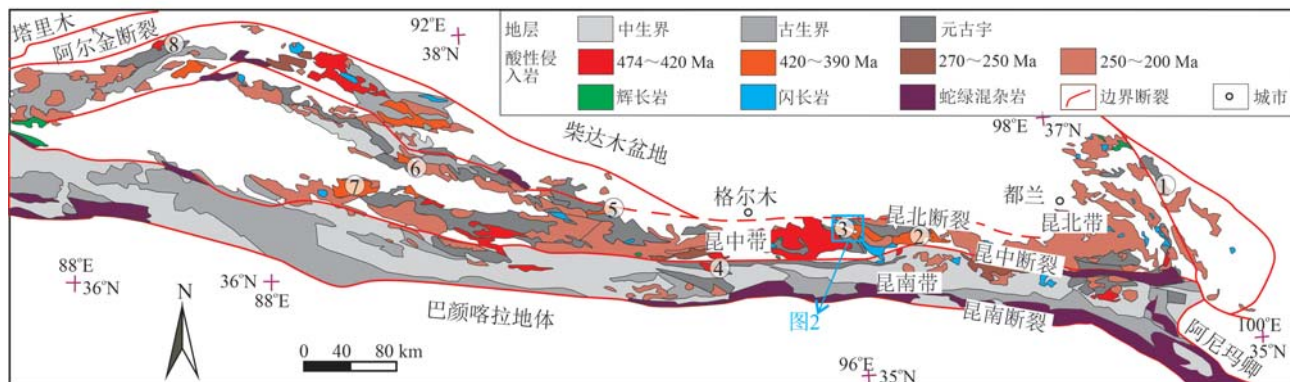


图1 东昆仑造山带地质图[据 Dong 等(2018)和 Wang 等 (2024)修编]

Fig. 1 The geological map of the East Kunlun Orogen (modified after Dong et al., 2018 and Wang et al., 2024)

- ①—呼德生 A2 型花岗岩(414 Ma, 曹锦山等, 2023); ②—冰沟 A2 型花岗岩(391 Ma, 刘彬等, 2013); ③—五龙沟 A型、I型花岗岩(427~414 Ma, Zhang et al., 2021); ④—万宝沟 A型花岗岩(441 Ma, 王晓霞等, 2012); ⑤—夏日哈木 A2 型花岗岩(391 Ma, 王冠等, 2013); ⑥—喀雅克登塔格 A型、I型花岗岩(424~394 Ma, Zhang et al., 2021); ⑦—卡尔却卡 A2 型花岗岩(425 Ma, 陈海福等, 2021); ⑧—白干湖 S型、A型花岗岩(432~414 Ma, Zhou et al., 2016; Zheng et al., 2018)
- ①—Hudesheng A2-type granite (414 Ma, Cao Jinshan et al., 2023); ②—Binggou A2-type granite (391 Ma, Liu Bin et al., 2013); ③—Wulonggou A-, I-type granite (427~414 Ma, Zhang et al., 2021); ④—Wanbaogou A-type granite (441 Ma, Wang Xiaoxia et al., 2012); ⑤—Xiarihamu A2-type granite (391 Ma, Wang Guan et al., 2013); ⑥—Kayakedengtage A-, I-type granite (424~394 Ma, Zhang et al., 2021); ⑦—Kaerqueka A2-type granite (425 Ma, Chen Haifu et al., 2021); ⑧—Baiganhu S-, A-type granite (432~414 Ma, Zhou et al., 2016; Zheng et al., 2018)

留纪和三叠纪蛇绿岩残块,昆南断裂带出现寒武纪、奥陶纪和石炭纪蛇绿岩残块(姜春发等, 1992; Dong et al., 2018; 裴先治等, 2018)。

东昆仑造山带志留纪-泥盆纪侵入岩以早期主要是 I 型或 S 型、晚期主要是 A 型为特征 (Zhang et al., 2021)。早期 I 型侵入岩主要出现在昆北带的西段和昆中以及昆南带的东段(图 1), 昆北带主要以闪长岩、花岗闪长岩和二长花岗岩为主, 岩体的锆石 U-Pb 年龄为 520~414 Ma (Yu et al., 2017; 王秉璋等, 2021); 昆中带和昆南带则以辉长岩、闪长岩、石英闪长岩、花岗闪长岩、二长花岗岩和正长花岗岩为主, 岩体的锆石 U-Pb 年龄为 515~436 Ma (Zhang et al., 2021); 晚期的 A 型花岗岩最早出现在万宝沟地区(441 Ma, 王晓霞等, 2012), 持续到中泥盆世(图 1), 见于夏日哈木(391 Ma, 王冠等, 2013)和五龙沟地区(390 Ma, 胡继春等, 2017)。最早出现的万宝沟 A 型花岗岩见环斑结构(441 Ma, 王晓霞等, 2012), 稍晚出现的 A 型花岗岩旁见少量略早的 S 型花岗岩(432 Ma, Zheng et al., 2018)和略晚的 I 型花岗岩(403 Ma, Zhang et al., 2021)。

五龙沟矿集区位于昆中带东段(图 1), 出露的岩体主要为加里东期和印支期, 大致以萤石沟-红旗沟韧性剪切带为界, 该剪切带及其南侧主要为加里东期正长花岗岩和花岗闪长岩, 年龄集中在 427~

410 Ma(图 2), 北侧主要为印支期花岗闪长岩和花岗岩, 年龄集中在约 240 Ma (Wang et al., 2024)。目前关于加里东期侵入岩的研究集中于矿集区中部, 其中水闸东沟-黄龙沟(亦称深水潭)北侧的二长花岗岩形成于早志留世(439 Ma, 王涛等, 2016), 此处花岗闪长岩(陆露等, 2013)和红旗沟沟口正长花岗岩(陆露等, 2013; 王艺龙等, 2018)则集中于 420~417 Ma, 糜棱岩化的碱性花岗岩形成于中泥盆世(390 Ma, 胡继春等, 2017); 水闸西沟和水闸东沟处的正长花岗岩则形成于晚志留世-早泥盆世(427~414 Ma, Zhang et al., 2021), 萤石沟花岗闪长岩则形成于早泥盆世(403 Ma, Zhang et al., 2021)。此外, 在萤石沟-红旗沟韧性剪切带及其北侧见晚志留世-早泥盆世的辉长岩(王艺龙等, 2018)。

2 岩体地质及岩相学特征

百吨沟花岗岩分布于东昆仑造山带东段五龙沟矿集区南部, 总体呈北西-南东向带状分布, 北西侧尖灭于红石岭和红旗沟南部, 南东至百吨沟以南约 5 km, 出露面积约 20 km²(图 2)。该岩体侵入古元古界金水口群中, 被晚古生代-中生代的岩体呈超动式侵入; 岩体被控矿的北西-南东向脆韧性剪切带切过, 闪长岩脉较发育。

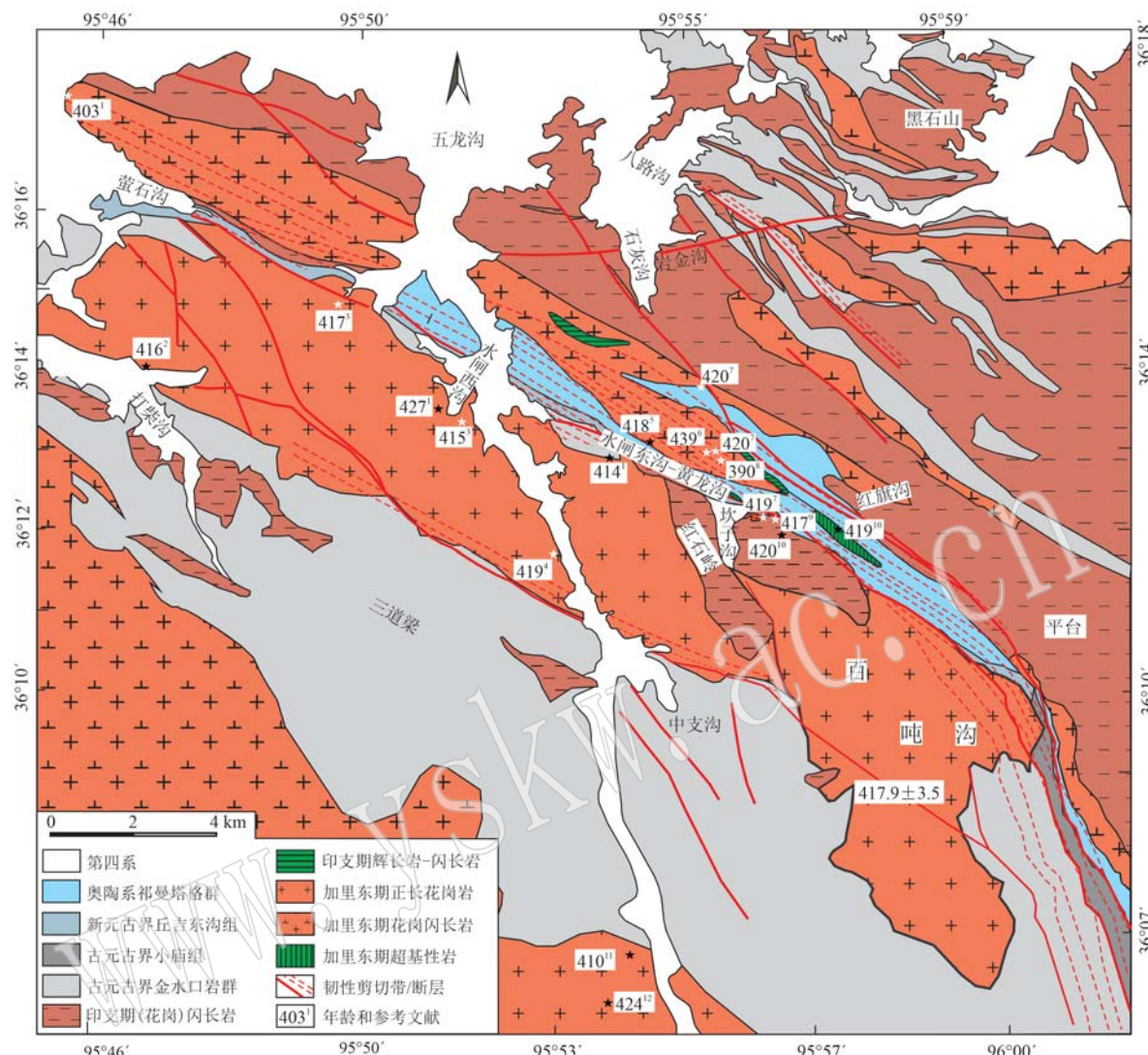


图2 五龙沟地区地质简图[据 Wang 等(2024)修改]

Fig. 2 Geological map of Wulonggou area(modified after Wang et al., 2024)

岩体年龄数据来源文献:1—Zhang et al., 2021; 2—Wang Tong, 2015; 3—Ding et al., 2019; 4—Yan Wei et al., 2016; 5—Wang Tao et al., 2016; 6—Chen et al., 2020; 7—Lu Lu et al., 2013; 8—Hu Jichun et al., 2017; 9—Li Xi, 2014; 10—Wang Yilong et al., 2018; 11—Zhang Liang et al., 2021; 12—Xin et al., 2018
References: 1—Zhang et al., 2021; 2—Wang Tong, 2015; 3—Ding et al., 2019; 4—Yan Wei et al., 2016; 5—Wang Tao et al., 2016; 6—Chen et al., 2020; 7—Lu Lu et al., 2013; 8—Hu Jichun et al., 2017; 9—Li Xi, 2014; 10—Wang Yilong et al., 2018; 11—Zhang Liang et al., 2021; 12—Xin et al., 2018

百吨沟花岗岩岩体岩性单一,为块状浅肉红色中粗粒花岗岩(图3)。采样时,所取样品尽量远离韧性剪切带,无明显蚀变,尽量选取矿物含量有区别的样品进行全岩地球化学分析。本次用于定年的样品采自岩体东部(百吨沟金狼沟,W03),岩石呈肉红色,块状构造,主要由钾长石(含量65%)和石英(含量25%)组成,见少量斜长石(含量5%),可见黑云母、萤石和铁氧化物等。钾长石呈他形板粒状,具条纹结构,主要为条纹长石,与石英呈文象状交生,钾长石部分发生轻微-中等程度土化,表面较脏(图

3c);石英较新鲜,在岩石中主要呈象形文字状交代钾长石产出,构成文象结构,少量呈他形不规则粒状分布于二者之间;斜长石呈他形板粒状,具较清晰的聚片双晶(图3d),后期部分发生轻微绢云母化、黏土化蚀变,分散状镶嵌分布;黑云母呈片状、鳞片状,后期发生脱铁蚀变绢云母化,零星分布于钾长石或石英间隙;金属矿物(包括铁质粉末)呈隐晶质集合体,主要为黑云母后期脱铁蚀变生成,分布于黑云母中;萤石呈他形粒状,糙面显著,见两组菱形解理,全消光,局部零星分布于岩石缝隙、裂隙之间。

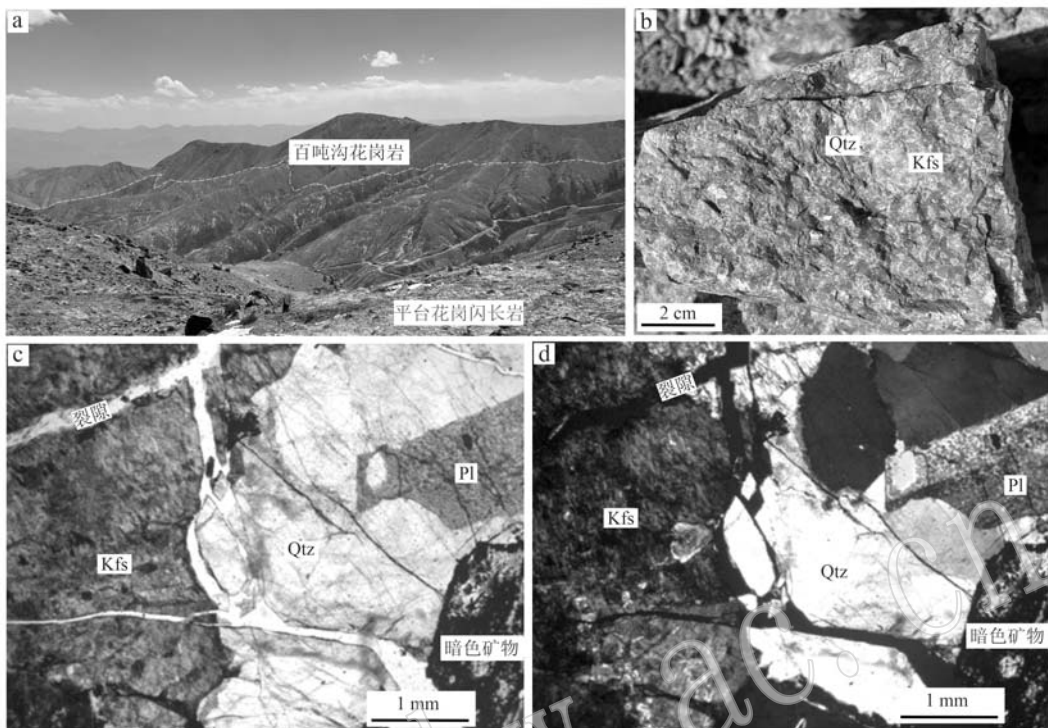


图3 百吨沟岩体野外(a)、标本(b)和岩相学(c为单偏光, d为正交偏光)特征

Fig. 3 Field (a), sample (b) and petrographic (c is polarized light, d is cross-polarized light) characteristics of Baidungou intrusion
 Pl—斜长石; Kfs—钾长石; Qtz—石英
 Pl—plagioclase; Kfs—potash feldspar; Qtz—quartz

3 测试方法

3.1 锆石 U-Pb 定年及 Hf 同位素分析

花岗岩样品(W03)锆石的分选、U-Pb 定年及 Hf 同位素分析在北京科融恩科技有限责任公司完成。锆石 U-Pb 定年用 LA-ICP-MS 完成, 激光剥蚀系统为 ESI NWR UP213 Nd: YAG 激光, ICP-MS 为 Agilent 7900 等离子体质谱仪。本次分析激光剥蚀斑束直径为 30 μm , 频率为 10 Hz; 单个样品点数据分析包括 20 s 仪器背景信号及 40 s 样品信号采集。分析方法详见包长甲等 (2021)。

锆石 Hf 同位素分析用 LA-MC-ICP-MS 完成, 采用飞秒激光剥蚀系统 ASI J200 和 MC-ICP-MS: ThermoFisher Neptune Plus 联用, 分析激光剥蚀斑束为 40 μm , 频率为 10 Hz, 每个分析点的数据包含 30 s 样品信号, 分析方法详见包长甲等 (2021)。Hf 一阶段和 Hf 二阶段模式年龄以及 $\varepsilon_{\text{Hf}}(t)$ 值的计算, 衰变常数 $\lambda = 1.867 \times 10^{-11}$, 现今球粒陨石的 $^{176}\text{Lu}/^{177}\text{Hf}$ 值

和 $^{176}\text{Hf}/^{177}\text{Hf}$ 值分别为 0.033 2 和 0.282 772, 亏损地幔的 $^{176}\text{Lu}/^{177}\text{Hf}$ 值和 $^{176}\text{Hf}/^{177}\text{Hf}$ 值分别为 0.038 40 和 0.283 25

3.2 全岩主微量元素分析

花岗岩经过切割, 选取无风化、无蚀变的新鲜岩块, 经过粉碎, 烘干等前处理, 在北京科融恩科技有限责任公司完成全岩主微量元素含量分析。主量元素采用 X 射线荧光光谱(XRF)进行分析, 分析精度优于 3%; 稀土和微量元素利用酸溶法制备样品, 用电感耦合等离子体质谱仪(Agilent 7900 ICP-MS)完成测试, 分析精度优于 5%。

4 分析结果

4.1 锆石年龄及 Hf 同位素特征

百吨沟花岗岩(W03)的锆石多为无色, 晶体大多较为自形, 呈短柱状-等轴状, 锆石颗粒约 100 μm , 定年结果及部分微量元素见表 1。所有锆石的 Th/U 值集中于 0.4~0.8, 显示出岩浆锆石 Th/U 值大于 0.4

表1 百吨沟花岗岩(W03) LA-ICP-MS 锆石U-Pb定年结果
Table 1 LA-ICP-MS zircon U-Pb dating results of Baidungou granite (W03)

点号	$w_{\text{B}}/10^{-6}$			Th/U			$^{207}\text{Pb}/^{206}\text{Pb}$			同位素比值			年龄/Ma			
	Pb	Th	U	$^{207}\text{Pb}/^{206}\text{Pb}$	$\pm 1\sigma$	$^{207}\text{Pb}/^{235}\text{U}$	$\pm 1\sigma$	$^{206}\text{Pb}/^{238}\text{U}$	$\pm 1\sigma$	$^{207}\text{Pb}/^{206}\text{Pb}$	$\pm 1\sigma$	$^{207}\text{Pb}/^{235}\text{U}$	$\pm 1\sigma$	$^{206}\text{Pb}/^{238}\text{U}$	$\pm 1\sigma$	
W03-01	42.0	214	512	0.42	0.0556	0.0013	0.5159	0.0135	0.0673	0.0016	435	52	422	9.1	420	9.3
W03-02	35.2	189	422	0.45	0.0569	0.0014	0.5323	0.0139	0.0679	0.0016	486	52	433	9.2	423	9.4
W03-03	31.9	163	388	0.42	0.0550	0.0014	0.5112	0.0140	0.0675	0.0016	410	55	419	9.4	421	9.4
W03-04	51.8	246	582	0.42	0.0618	0.0017	0.6097	0.0174	0.0716	0.0017	666	56	483	11	446	10
W03-05	40.7	302	465	0.65	0.0548	0.0013	0.5115	0.0133	0.0677	0.0016	405	52	419	8.9	422	9.4
W03-06	12.2	68	145	0.47	0.0598	0.0021	0.5576	0.0203	0.0677	0.0016	595	75	450	13	422	9.7
W03-07	22.4	122	272	0.45	0.0556	0.0015	0.5152	0.0151	0.0673	0.0016	434	60	422	10	420	9.4
W03-08	44.1	210	540	0.39	0.0573	0.0013	0.5331	0.0136	0.0675	0.0016	501	51	434	9.0	421	9.4
W03-09	42.3	239	515	0.46	0.0556	0.0014	0.5123	0.0136	0.0669	0.0015	436	53	420	9.1	417	9.3
W03-10	18.0	105	216	0.49	0.0608	0.0019	0.5550	0.0178	0.0662	0.0016	631	65	448	12	413	9.4
W03-11	26.9	138	322	0.43	0.0582	0.0021	0.5403	0.0197	0.0674	0.0016	535	76	439	13	420	9.7
W03-12	19.1	93	235	0.4	0.0557	0.0017	0.5131	0.0160	0.0669	0.0016	439	64	421	11	417	9.4
W03-13	33.5	210	404	0.52	0.0573	0.0016	0.5251	0.0151	0.0664	0.0015	504	59	429	10	415	9.3
W03-14	42.5	292	500	0.58	0.0556	0.0013	0.5138	0.0135	0.0671	0.0015	435	53	421	9.1	418	9.3
W03-15	32.8	265	369	0.72	0.0562	0.0019	0.5208	0.0181	0.0672	0.0016	461	73	426	12	419	9.6
W03-16	32.9	184	402	0.46	0.0563	0.0016	0.5150	0.0158	0.0663	0.0015	465	64	422	11	414	9.3
W03-17	34.9	172	430	0.4	0.0568	0.0016	0.5219	0.0157	0.0667	0.0016	482	62	426	11	416	9.4
W03-18	52.4	286	647	0.44	0.0560	0.0014	0.5106	0.0134	0.0661	0.0015	453	53	419	9.0	413	9.2
W03-19	34.5	213	409	0.52	0.0574	0.0015	0.5318	0.0146	0.0672	0.0016	507	55	433	9.7	419	9.4
W03-20	29.4	210	341	0.62	0.0554	0.0015	0.5164	0.0146	0.0676	0.0016	430	57	423	9.8	421	9.4
W03-21	24.1	141	295	0.48	0.0564	0.0015	0.5132	0.0150	0.0660	0.0015	468	60	421	10	412	9.2
W03-22	23.3	127	279	0.46	0.0569	0.0020	0.5282	0.0194	0.0673	0.0016	488	78	431	13	420	9.7
W03-23	54.3	302	672	0.45	0.0572	0.0013	0.5168	0.0133	0.0655	0.0015	499	51	423	8.9	409	9.1
W03-24	41.1	221	501	0.44	0.0560	0.0014	0.5161	0.0139	0.0668	0.0015	454	54	423	9.3	417	9.3
W03-25	46.6	228	572	0.4	0.0575	0.0015	0.5272	0.0146	0.0665	0.0015	509	56	430	9.7	415	9.3
W03-26	28.7	199	335	0.59	0.0560	0.0016	0.5183	0.0158	0.0671	0.0016	452	63	424	11	419	9.4
W03-27	46.5	374	515	0.73	0.0574	0.0016	0.5424	0.0158	0.0686	0.0016	505	59	440	10	428	9.6
W03-28	40.8	267	490	0.54	0.0582	0.0020	0.5251	0.0184	0.0654	0.0016	538	73	429	12	408	9.4
W03-29	37.4	224	442	0.51	0.0583	0.0015	0.5412	0.0146	0.0674	0.0016	540	54	439	9.6	420	9.4
W03-30	42.5	409	458	0.89	0.0562	0.0016	0.5236	0.0159	0.0675	0.0016	461	63	428	11	421	9.5

的特征(吴元保等, 2004)。剥蚀的30颗锆石中有1颗表面年龄为 446 ± 10 Ma(图4a), 且谐和度较差, 剩余29颗集中于420 Ma(图4a)。对这些谐和数据点进行计算, 获得 $^{206}\text{Pb}/^{238}\text{U}$ 加权平均年龄为 417.9 ± 3.5 Ma(MSWD=0.21, $n=29$)。

对颗粒形态较好、环带清晰且已获得年龄的锆石进行原位Hf同位素分析, 分析结果见表2。所有

测试点的Hf同位素组成较一致, $^{176}\text{Lu}/^{177}\text{Hf}$ 值小于0.002, 说明锆石形成后基本没有放射性成因Hf累积, 其 $^{176}\text{Hf}/^{177}\text{Hf}$ 值可用来分析源区特征。10个点的 $^{176}\text{Hf}/^{177}\text{Hf}$ 值介于0.282 509~0.282 577之间, 以对应的锆石U-Pb年龄计算出的 $\varepsilon\text{Hf}(t)$ 值介于-0.6~1.9之间, 二阶段Hf模式年龄 $t_{2\text{DM}}$ 介于1 442~1 284 Ma之间, 远大于锆石结晶的年龄。

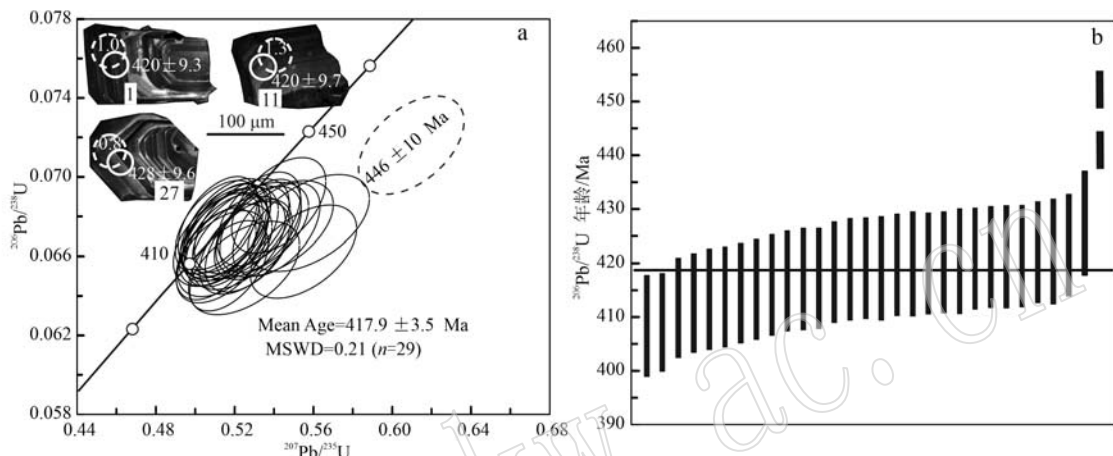


图4 百吨沟花岗岩锆石CL(a)和U-Pb年龄图(b)

Fig. 4 Zircon CL (a) and U-Pb age diagram (b) of Baidungou granite

锆石CL图像中实线圆圈为测年位置, 虚线圆圈为Hf同位素分析位置

the solid-line circles are the U-Pb dating positions, the dashed line circles are the Hf isotope analysis positions

表2 百吨沟花岗岩(W03)锆石Hf同位素分析结果

Table 2 Zircon Hf dating results of Baidungou granite (W03)

点号	年龄/Ma	$^{176}\text{Yb}/^{177}\text{Hf}$	$\pm 2\sigma$	$^{176}\text{Lu}/^{177}\text{Hf}$	$\pm 2\sigma$	$^{176}\text{Hf}/^{177}\text{Hf}$	$\pm 2\sigma$	$\varepsilon\text{Hf}(t)$	t_{DM}/Ma	$t_{2\text{DM}}/\text{Ma}$	$f_{\text{Lu/Hf}}$
W03-1	420	0.036 041	0.000 216	0.001 210	0.000 009	0.282 548	0.000 019	1.0	1 002	1 344	-0.96
W03-5	422	0.047 365	0.000 215	0.001 516	0.000 015	0.282 528	0.000 028	0.2	1 039	1 394	-0.95
W03-6	422	0.030 855	0.001 104	0.001 053	0.000 018	0.282 528	0.000 021	0.4	1 025	1 385	-0.97
W03-10	413	0.038 683	0.001 675	0.001 293	0.000 029	0.282 555	0.000 018	1.1	994	1 334	-0.96
W03-11	420	0.022 793	0.000 949	0.000 786	0.000 015	0.282 552	0.000 016	1.3	984	1 327	-0.98
W03-13	415	0.035 911	0.000 452	0.001 278	0.000 008	0.282 577	0.000 019	1.9	963	1 284	-0.96
W03-15	419	0.050 653	0.001 787	0.001 696	0.000 070	0.282 515	0.000 017	-0.3	1 061	1 427	-0.95
W03-26	419	0.050 318	0.000 910	0.001 738	0.000 014	0.282 509	0.000 019	-0.6	1 072	1 442	-0.95
W03-27	428	0.031 357	0.000 238	0.001 029	0.000 018	0.282 536	0.000 014	0.8	1 014	1 364	-0.97
W03-30	421	0.060 149	0.002 287	0.001 912	0.000 039	0.282 535	0.000 017	0.4	1 039	1 385	-0.94

4.2 全岩主微量元素特征

百吨沟岩体主微量元素结果见表3, 该岩体 SiO_2 含量介于71.2%~77.2%之间, Na_2O 含量分布于3.37%~5.46%之间, K_2O 含量集中在4.32%~5.26%之间, 对应的 $\text{K}_2\text{O}/\text{Na}_2\text{O}$ 值为0.95~1.55, $\text{K}_2\text{O}+\text{Na}_2\text{O}$ 为8.23%~10.70%; 同时, 岩体 Al_2O_3 含量在11.9%~15.7%之间, CaO 含量介于0.09%~

0.95%之间, MgO 含量为0.04%~0.22%。样品的A/CNK值为0.99~1.15, 属于准铝质-弱过铝质序列。在 $\text{Na}_2\text{O}+\text{K}_2\text{O}-\text{SiO}_2$ 图解上, 样品落入花岗岩区域(图5a), 在 $\text{K}_2\text{O}-\text{SiO}_2$ 图解中显示样品多具有高钾钙碱性特征(图5b)。

百吨沟岩体的稀土元素总含量介于 179×10^{-6} ~ 526×10^{-6} 之间, $(\text{La}/\text{Yb})_N$ 值介于0.84~19.20之

表3 百吨沟花岗岩全岩主量($w_B/\%$)、微量元素和稀土元素含量($w_B/10^{-6}$)表Table 3 Main ($w_B/\%$), trace and rare earth element ($w_B/10^{-6}$) contents of the whole rock of the Baidungou granite

采样位置 样品	五龙沟						采样位置 样品	金狼沟					
	W02	W03	W11	W12	W13	W14		W02	W03	W11	W12	W13	W14
SiO ₂	73.8	73.1	72.1	71.2	75.7	77.2	Ba	16.0	214.0	246.0	37.8	30.6	17.8
TiO ₂	0.12	0.16	0.28	0.07	0.06	0.07	La	104.0	66.6	82.2	17.8	20.7	24.2
Al ₂ O ₃	13.4	13.5	14.7	15.7	13.5	11.9	Ce	217.0	132.0	165.0	52.3	62.3	61.8
TFe ₂ O ₃	1.55	1.44	1.87	0.94	0.37	0.90	Pr	25.80	15.00	18.60	7.55	10.20	7.25
MnO	0.02	0.01	0.02	0.003	0.002	0.01	Nd	95.5	51.1	68.4	34.6	54.5	29.7
MgO	0.04	0.06	0.22	0.05	0.04	0.06	Sm	17.6	8.37	12.1	12.9	27.4	8.8
CaO	0.47	0.95	0.29	0.47	0.33	0.50	Eu	0.06	0.28	0.41	0.04	0.08	0.07
Na ₂ O	3.79	3.37	3.97	5.46	4.34	3.91	Gd	17.0	7.26	10.2	16.2	51.2	10.9
K ₂ O	5.24	5.23	5.26	5.20	4.58	4.32	Tb	3.30	1.08	1.52	3.13	10.20	2.08
P ₂ O ₅	0.01	0.01	0.03	0.01	0.003	0.01	Dy	18.80	4.99	7.75	19.70	60.90	13.20
烧失量	1.39	2.08	1.11	0.80	0.95	0.98	Ho	3.63	0.92	1.46	4.10	10.70	2.69
总和	98.4	97.8	99.9	99.8	99.8	99.9	Er	10.70	2.70	3.90	12.50	23.40	7.71
K ₂ O/Na ₂ O	1.38	1.55	1.33	0.95	1.06	1.10	Tm	1.6	0.43	0.58	2.17	3.06	1.21
Na ₂ O+K ₂ O	9.03	8.61	9.23	10.70	8.92	8.23	Yb	9.53	2.49	3.75	15.20	17.50	7.69
A/CNK	1.05	1.04	1.15	1.01	1.06	0.99	Lu	1.44	0.40	0.59	2.75	2.46	1.28
A/NK	1.13	1.20	1.20	1.07	1.11	1.07	Hf	17.30	8.58	9.93	16.20	9.10	17.50
$t_{Zr}/^{\circ}\text{C}$	896	836	826	816	778	827	Ta	1.88	1.48	1.22	2.76	2.54	3.15
Li	7.18	3.47	12.1	5.45	5.43	9.70	Pb	34.7	19.0	22.9	36.9	35.7	17.2
Be	2.47	1.63	2.69	6.29	4.36	3.63	Th	40.4	21.6	29.3	67.9	49.0	41.5
Sc	0.59	1.93	3.62	1.38	0.84	0.61	U	9.39	5.57	4.05	16.50	13.90	14.60
V	1.05	3.57	8.17	3.17	2.50	1.97	10 000 Ga/Al	36.90	27.90	3.39	3.77	3.73	4.71
Cr	0.66	1.66	14.3	18.6	14.7	13.9	Y+Nb	142.0	38.8	54.7	163.0	316.0	102.0
Co	0.05	0.50	1.36	0.17	0.15	0.12	Nb/Ta	12.90	7.50	14.80	9.76	8.22	9.66
Ni	-	0.17	1.28	0.88	0.80	0.84	ΣREE	526	294	376	201	355	179
Cu	8.05	4.73	2.87	2.33	1.75	65.1	LREE	460	274	346	125	175	132
Zn	82.1	31.5	33.4	55.9	21.1	82.8	HREE	66.0	20.3	29.7	75.8	179.0	46.8
Ga	22.3	15.9	26.3	31.2	26.5	29.7	LREE/HREE	6.97	13.50	11.70	1.65	0.98	2.82
Rb	262	200	234	503	430	476	(La/Sm) _N	3.82	5.14	4.37	0.89	0.49	1.78
Sr	7.70	28.00	35.50	13.10	9.98	5.56	(Gd/Yb) _N	1.47	2.41	2.24	0.88	2.43	1.17
Y	119.0	27.7	36.7	136.0	295.0	71.1	(La/Yb) _N	7.82	19.20	15.70	0.84	0.85	2.26
Zr	458	234	229	252	140	257	Eu/Eu [*]	0.01	0.11	0.11	0.01	0.01	0.02
Nb	24.2	11.1	18.0	27.0	20.9	30.5	R_1	2 340	2 460	2 141	1 579	2 449	2 750
Sn	6.92	6.13	5.43	13.30	16.10	10.20	R_2	320	378	334	363	304	294
Cs	3.14	3.06	3.18	7.15	4.94	6.04							

注: - 表示低于检测限; A/CNK=Al₂O₃/CaO+Na₂O+K₂O(摩尔比); $t_{Zr}=12 900/(2.95+0.85M+\ln D_{Zr})$, 其中 M=(Na⁺+K⁺+2 Ca²⁺)/(Al³⁺Si⁴⁺), D_{Zr} 为饱和熔体Zr含量与锆石Zr含量(496 000×10⁻⁶)的比值; $R_1=4 Si-11(Na+K)-2(Fe+Ti)$, $R_2=6 Ca+2 Mg+Al$ 。

间, LREE/HREE 值在 0.98~13.50 之间变化, 反映较强的轻、重稀土元素分馏特征。 $(\text{La}/\text{Sm})_N$ 值在 0.49~5.14 之间, $(\text{Gd}/\text{Yb})_N$ 值在 0.88~2.43 之间, 表明岩石具有较平坦的重稀土元素配分模式; 样品具有弱或明显的 Eu 负异常(0.01~0.11), 球粒陨石标准化稀土元素配分模式表现为轻稀土元素较为富集、重稀土元素略微亏损的略向右倾的特征(图 6a)。

在原始地幔标准化微量元素蛛网图中, 百吨沟岩体普遍富集 Rb、Th、U、Ta、Pb、Nd 等元素, 亏损 Ba、Nb、Sr、P、Ti 等元素(图 6b), 样品 Nb/Ta 值介于

7.5~14.8 之间, 低于地幔平均值(17.7), 接近地壳平均值(11)。

5 讨论

5.1 岩石类型和成因

ISMA 是花岗岩最常用的分类方法, 其中 ISM 型是基于岩浆源区性质的划分, I 型和 S 型分别来自(变质)火成岩和沉积岩, M 型来自于地幔(陈建林等, 2004), 而 A 型则是指碱性、无水和非造山环境的花岗岩(Loiselle and Wones, 1979)。ISMA 的分类

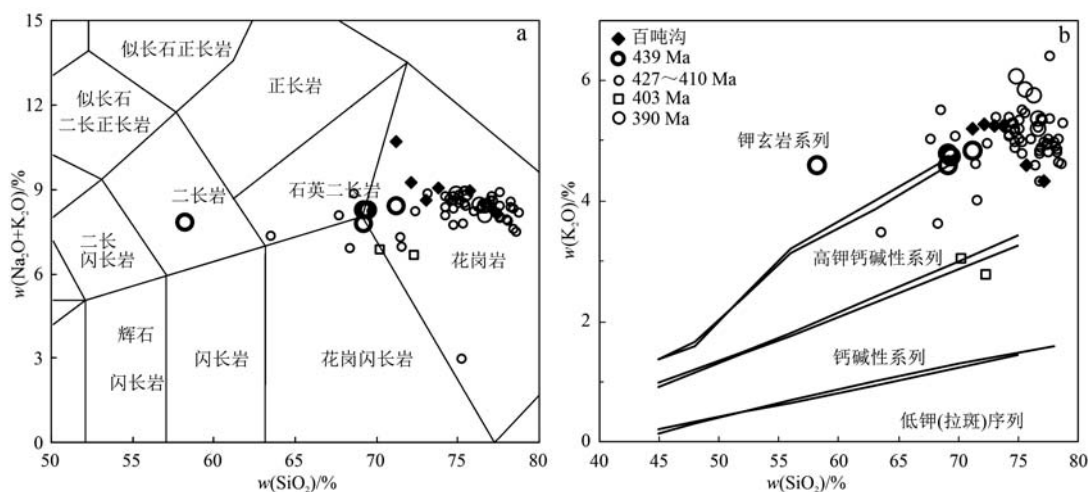


图 5 百吨沟花岗岩 TAS(a, 底图据 Middlemost, 1994) 和 K_2O - SiO_2 (b, 底图据 Peccerillo and Taylor, 1976 和 Middlemost, 1985) 图解

Fig. 5 Discrimination diagrams of TAS (a, Middlemost, 1994) and K_2O - SiO_2 (b, Peccerillo and Taylor, 1976; Middlemost, 1985) of Baidungou granite

其他花岗岩数据来源:红旗沟(王艺龙等, 2018),三道梁南(张亮等, 2021),黑石沟、打柴沟、水闸东沟(王铜, 2015; 王涛等, 2016),淡水沟和深水潭(Chen et al., 2020),石洞沟和水闸西沟(Ding et al., 2019),猴头沟(严威等, 2016),水闸西沟-水闸东沟(Zhang et al., 2021) other granite data in Wulonggou area are from: Hongqigou (Wang Yilong et al., 2018), Sandaoliangnan (Zhang Liang et al., 2021), Heishigou, Dachaigou and Shuizhadonggou (Wang Tong, 2015; Wang Tao et al., 2016), Danshuigou and Shenshuitan (Chen et al., 2020), Shidonggou and Shuizhaxigou (Ding et al., 2019), Houtougou (Yan Wei et al., 2016), Shuizhaxigou-Shuizhadonggou (Zhang et al., 2021)

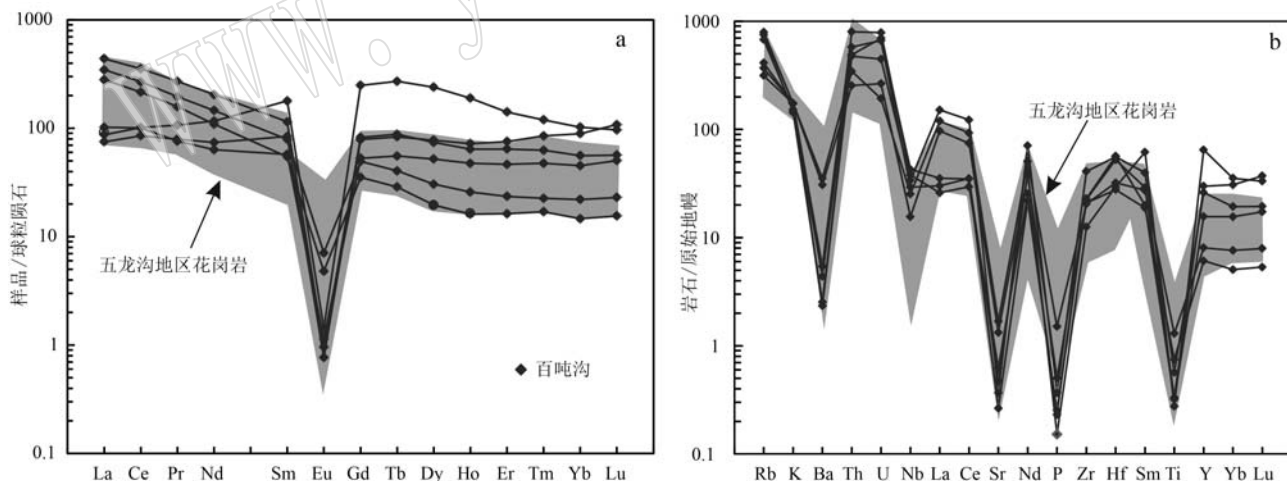


图 6 花岗岩球粒陨石标准化稀土元素配分模式(a)和原始地幔标准化微量元素蛛网图(b)(标准值据 Sun and McDonough (1989), 五龙沟地区花岗岩数据来源同图 5)

Fig. 6 Chondrite-normalized REE patterns (a) and primitive mantle-normalized trace element patterns (b) for granite (normalization value after Sun and McDonough, 1989; others granite data source in Wulonggou area is the same as Fig. 5)

中 M 型花岗岩 K_2O 含量一般低于 0.6% (马鸿文, 1992), 因此排除百吨沟花岗岩是 M 型。百吨沟花岗岩富 Nb、Ga 和 Y, 贫 Al、Mg 和 Ca 并且具有“海鸥型”稀土元素配分模式, 具有 A 型花岗岩的特征(贾小辉等, 2009; Frost and Frost, 2011)。

I&S 型与 A 型花岗岩的区分常使用全岩 Ga/Al 值(吴福元等, 2007), 在 $(Na_2O+K_2O)-10\,000\,Ga/Al$ 判别图解中, 百吨沟花岗岩落入 A 型花岗岩区域(图 7a), 指示其可能是 A 型。TFeO(全铁)含量是识别 A 型花岗岩的重要指标(>1%, 王强等, 2000), 百吨

沟花岗岩TFeO多大于1%,同时相比同时代的A型花岗岩,其具有较高的TFeO/MgO,在对应的判别图解中,有2/3的样品落在A型花岗岩及其与I&S型花岗岩界线附近(图7b),因此,百吨沟花岗岩应为A型。尽管高分异的I&S型也会出现高Ga/Al的特

征(吴福元等,2017),但高分异S型花岗岩具有富P低Na的特点,高分异I型全铁含量低于1%且Rb高于 270×10^{-6} (贾小辉等,2009),这些均与百吨沟花岗岩低P₂O₅(多小于0.01%)高TFeO(多大于1%)具有明显的区别。

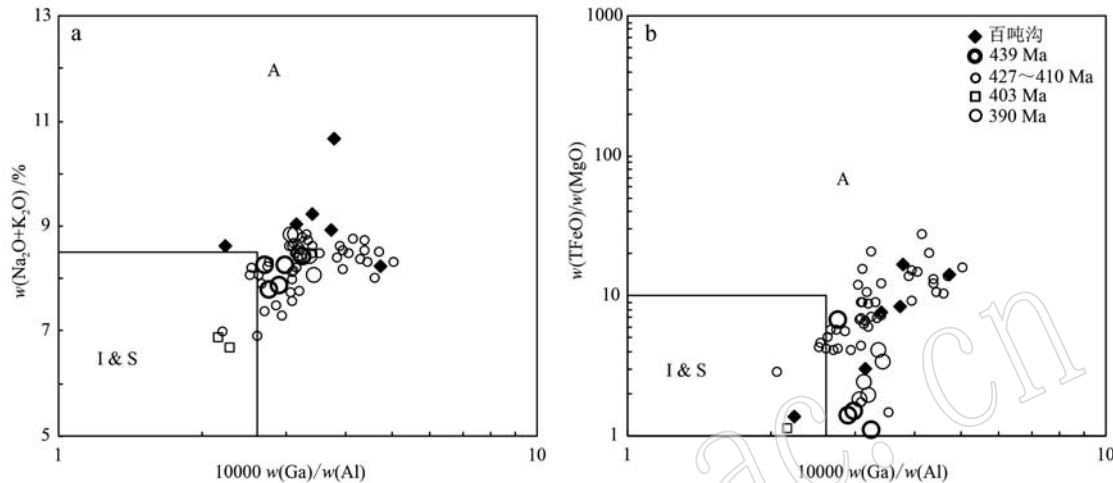


图7 花岗岩成因类型判别图解(底图据 Whalen *et al.*, 1987, 百吨沟以外的数据来源同图5)

Fig. 7 Discrimination diagrams of genetic type of granite (after Whalen *et al.*, 1987; the granite data source except Baidungou is the same as Fig. 5)

温度是A型花岗岩判别重要的标志(吴福元等,2007),大多数花岗质岩浆被认为是绝热上升就位的,其温度在岩浆早期结晶时与形成时近似(吴福元等,2007)。温度的计算常用锆石饱和温度计(Watson and Harrison, 1983; Miller *et al.*, 2003; 王帅等,2022),通过公式(Watson and Harrison, 1983)计算,百吨沟花岗岩锆石饱和结晶的温度为778~896°C(平均830°C)。当花岗岩含有大量(大于10%~50%)继承锆石时,锆石的饱和温度可能略高于岩浆源区的温度,而不含或只含少量继承锆石时,则相反(Miller *et al.*, 2003)。根据百吨沟花岗岩只含有少量(<10%)继承锆石核,其锆石饱和温度的平均值(830°C)应近似于岩浆源区的温度。该温度非常接近A型花岗岩的温度(839°C, King *et al.*, 1997),且明显高于高分异花岗岩形成的温度(764°C, King *et al.*, 1997),因此认为百吨沟花岗岩是A型花岗岩。

目前关于A型花岗岩的成因模式主要有幔源玄武岩的分离结晶、长英质地壳岩石的部分熔融及其这两种模式的结合(Frost and Frost, 2011)。幔源岩浆分离结晶形成的A型花岗岩会伴随大规模同时期的基性-超基性岩(Turner *et al.*, 1992),而五龙沟地

区仅在红旗沟一带见少量带状分布的基性-超基性岩(王艺龙等,2018);岩浆混合形成的A型花岗岩会含有大量暗色微粒包体并且显示出变化较大的Hf同位素特征(Yang *et al.*, 2006),这也与百吨沟岩体的特征相矛盾(图8)。百吨沟花岗岩具有较低的Nb/U和Ce/Pb值,分别为1.50~4.45(平均值为2.37)和1.42~7.19(平均值为4.53),与原始地幔的Nb/U和Ce/Pb值(平均值分别约30和9)相差较大,而与平均地壳的Nb/U和Ce/Pb值(平均值分别约10和4)相近(Hofmann *et al.*, 1986),反映其主要来源于长英质地壳岩石的部分熔融。

新生的基性下地壳、花岗质熔体抽离后无水的麻粒岩下地壳和浅部长英质岩石在部分熔融时均可以形成A型花岗岩(Xin *et al.*, 2018)。基性下地壳的部分熔融不能产生大量高硅(SiO₂>70%)的熔体(Rapp and Watson, 1995),一般产生准铝质且K₂O/Na₂O<1的花岗岩(Rapp and Watson, 1995);无水的麻粒岩下地壳部分熔融会产生低TiO₂/MgO和(Na₂O+K₂O)/Al₂O₃的熔体(Creaser *et al.*, 1991; Douce, 1997),均与百吨沟花岗岩高硅(SiO₂>71%)、更富钾(K₂O/Na₂O>1)、高TiO₂/MgO(平均值0.97)和高(Na₂O+K₂O)/Al₂O₃(平均值0.66)不同。

同时,百吨沟花岗岩亏损 Ba、Sr 等元素,反映其岩浆起源于残留或富集斜长石而无石榴子石残留的浅部低压区(Rapp and Watson, 1995),这与 Qz-Ab-Or 组分估算的酸性熔体形成压力一致(低于 0.5 GPa, 图 8),因此,排除新生的基性下地壳和麻粒岩下地壳作为岩浆源区的可能。

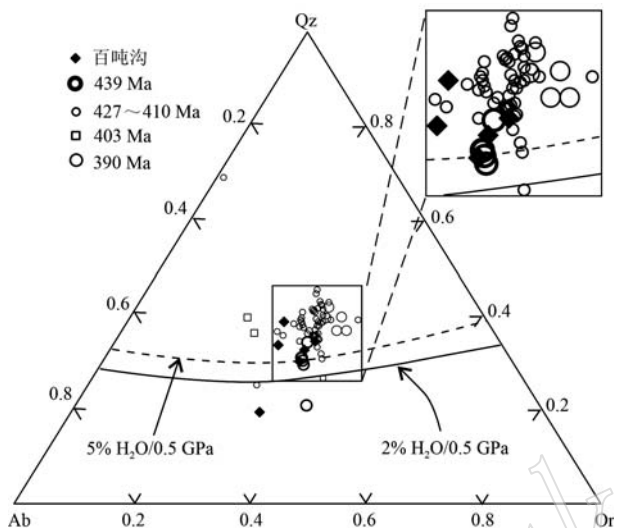


图 8 百吨沟花岗岩 Qz-Ab-Or 图(等压线据 Long *et al.*, 1986; 百吨沟以外的数据来源同图 5)

Fig. 8 Qz-Ab-Or diagram of the Baidungou granite (isoplestic lines after Long *et al.*, 1986; the granite data source except Baidungou is the same as Fig. 5)

长英质火成岩在高温低压下部分熔融形成的 A 型花岗岩具有准铝质-弱过铝质的特征(Frost and Frost, 2011),与百吨沟花岗岩性质一致。百吨沟花岗岩锆石的 $\varepsilon\text{Hf}(t)$ 值接近于 0 并且二阶段 Hf 模式年龄 t_{2DM} 介于 1 442~1 284 Ma 之间,反映其岩浆源区的长英质火成岩有新生组分的参与,最有可能来自于与之具有相似 Hf 同位素特征的与俯冲有关的闪长岩-花岗闪长岩(Xin *et al.*, 2018; Chen *et al.*, 2020)。相比于五龙沟地区其他近同时的花岗岩,百吨沟花岗岩锆石的 $\varepsilon\text{Hf}(t)$ 值变化小且较高(略大于 0 值,图 9),反映其岩浆源区更均一或受古老地壳物质的影响较小(Xin *et al.*, 2018; Chen *et al.*, 2020; Zhang *et al.*, 2021)或者有少量地幔物质的参与。少量幔源物质参与并不能排除的原因是高温的热源可能与地幔有关(Whalen *et al.*, 1987; Bonin, 2007),且五龙沟地区存在略晚的来自幔源的基性岩浆作用(王艺龙等, 2018)。此外,百吨沟花岗岩更亏损 P 和 Ti 等元素(图 6b)可能与更多的磷灰

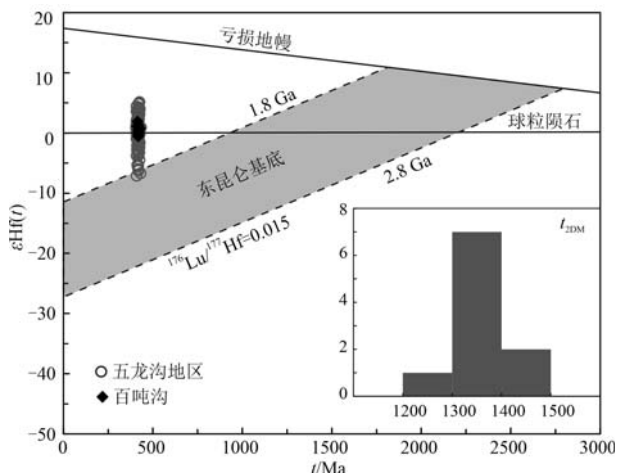


图 9 百吨沟花岗岩锆石 $\varepsilon\text{Hf}(t)$ - t 图解

Fig. 9 $\varepsilon\text{Hf}(t)$ - t diagram of zircon for Baidungou granite
五龙沟地区花岗岩锆石 Hf 同位素数据来源:红旗沟(王艺龙等, 2018),三道梁南(张亮等, 2021),淡水沟和深水潭(Chen *et al.*, 2020),石洞沟和水闸西沟(Ding *et al.*, 2019),猴头沟(严威等, 2016)

zircon Hf isotope data of granite in Wulonggou area are derived from: Hongqigou (Wang Yilong *et al.*, 2018), Sandaoliangnan (Zhang Liang *et al.*, 2021), Danshuigou and Shenshuitan (Chen *et al.*, 2020), Shidonggou and Shuihazigou (Ding *et al.*, 2019), Houtougou (Yan Wei *et al.*, 2016)

石和钛铁矿分离结晶有关。

5.2 构造意义

尽管东昆仑造山带原特提斯洋的俯冲极性存在着争议,但普遍认为与俯冲相关的钙碱性岩浆持续到约 430 Ma(Zhang *et al.*, 2021)。A 型花岗岩是判别伸展环境的重要标志(吴福元等, 2007),五龙沟地区除约 403 Ma 的花岗闪长岩是 I 型(403 Ma, Zhang *et al.*, 2021),其余花岗岩具有 A 型(图 7)且是 A2 型的特征(图 10)。尽管五龙沟地区所有的 A 型花岗岩在 Rb-(Y+Nb) 图解中投在后碰撞花岗岩区域(图 11a),但最早具有 A 型特征的二长花岗岩(439 Ma, 王涛等, 2016)并不能指示后碰撞的伸展环境。该二长花岗岩在 R_2-R_1 判别图中处于同碰撞环境,与五龙沟地区其他花岗岩具有明显的区别(图 11b),更为重要的是,造山带内稍晚出现的 S 型花岗岩(432 Ma, Zheng *et al.*, 2018)和榴辉岩峰期变质(约 432 Ma, 国显正等, 2018)反映约 439 Ma 时仍处于挤压环境。

五龙沟地区大量 A 型花岗岩集中出现在 427~410 Ma,但 427 Ma 的年龄仅在水闸西沟处出现,其余样品年龄集中在 420~414 Ma(图 2)。这些 A 型花

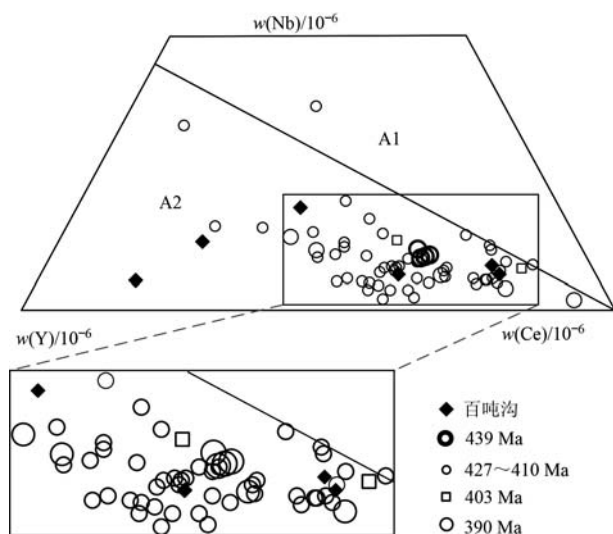


图 10 A型花岗岩构造环境判别图解(据 Eby, 1992);
百吨沟以外的数据来源同图 5)

Fig. 10 Discrimination diagram of tectonic environment of A-type granite (after Eby, 1992; the granite data source except Baidungou is the same as Fig. 5)

岗岩具有极其相似的主微量元素以及稀土元素特征(图 6),如果考虑 LA-ICP-MS 定年的误差(2RSD 约 4%, 李献华等, 2015),这些花岗岩可能形成于约 420 Ma, 仅仅略早于该地区来自于软流圈地幔或亏损地幔的基性岩(419 Ma, 王艺龙等, 2018)以及具有壳幔混合特征的 I 型花岗闪长岩(403 Ma, Zhang *et al.*, 2021)。结合李佳斌等(2023)在五龙沟旁侧发现麻粒岩相(年龄 411.4 ± 2.9 Ma)低压高温的变质条件指示软流圈地幔的上涌,可能反映五龙沟地区约 420 Ma 进入后碰撞伸展阶段。

磨拉石沉积以及区域韧性剪切常被用来限制碰撞时间的上限(李继亮等, 1999)。陆露等(2010)在格尔木水泥厂地区获得东昆仑造山带最早的磨拉石沉积年龄为 423.2 ± 1.8 Ma, 陈能松等(2007)在格尔木以东的清水泉一带获得云母片岩的变质年龄为 420 ± 20 Ma, 与韧性剪切带角闪石的 Ar-Ar 坪年龄(427 ± 5 Ma, 陈能松等, 2002)一致, 指示东昆仑造山

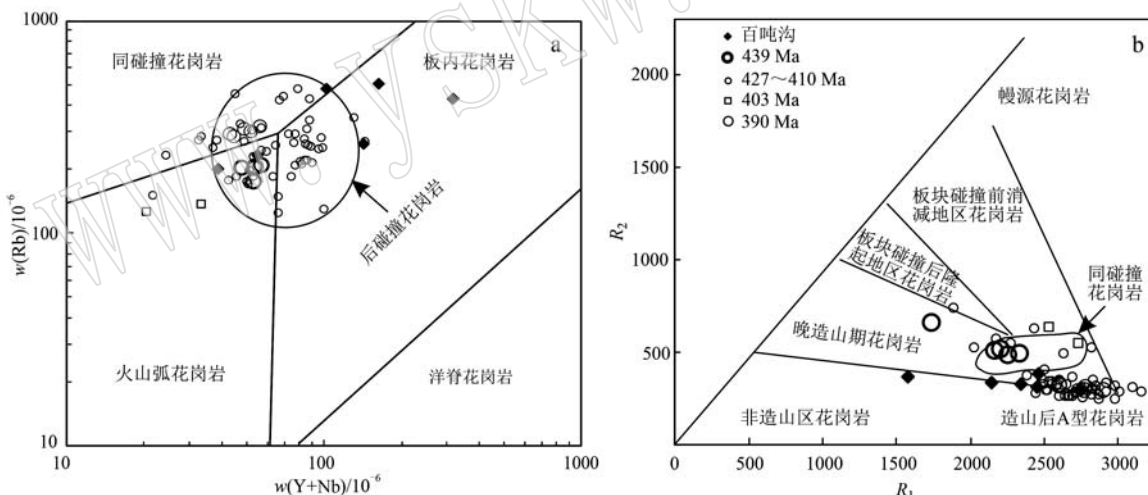


图 11 百吨沟花岗岩构造背景判别[a 和 b 底图分别据 Pearce (1996) 和 Batchelor and Bowden (1985), 百吨沟以外的数据来源同图 5]

Fig. 11 Discrimination of tectonic background of Baidungou granite (a and b is after Pearce, 1996 and Batchelor and Bowden, 1985, respectively; the granite data source except Baidungou is the same as Fig. 5)

带在约 420 Ma 碰撞结束,进入后碰撞的伸展阶段。因此,东昆仑造山带出现大量近同时($425 \sim 414$ Ma)的 A2 型花岗岩(图 1),指示整个造山带约 420 Ma 进入后碰撞阶段。

6 结论

(1) 百吨沟花岗岩的锆石 U-Pb 年龄为 417.9 ± 3.5 Ma, 为晚志留世-早泥盆世岩浆活动的产物。

(2) 岩石高硅、富碱,低镁、钙,富集大离子亲石元素和亏损高场强元素,具有明显的负铕异常和“海鸥型”稀土元素配分模式,具有较高的Ga/Al值和Zr饱和温度,其锆石 $\varepsilon\text{Hf}(t)$ 值介于-0.6~1.9之间,为A型花岗岩,推测其源于长英质火成岩的部分熔融。

(3) 岩石具有A2型花岗岩的特征,形成于后碰撞伸展的环境,指示东昆仑造山带在晚志留世时进入后碰撞伸展阶段。

References

- Bao Changjia, Chai Fengmei, Li Yong, et al. 2021. Geochronology and geochemical characteristics of granitoids in the bastille tungsten polymetallic deposit in the southern margin of Altay: Implications for tungsten mineralization [J]. *Acta Petrologica Sinica*, 37(3): 886~910 (in Chinese with English abstract).
- Batchelor R A and Bowden P. 1985. Petrogenetic interpretation of granitoid rock series using multicationic parameters [J]. *Chemical Geology*, 48(1~4): 43~55.
- Bonin B. 2007. A-type granites and related rocks: Evolution of a concept, problems and prospects [J]. *Lithos*, 97(1~2): 1~29.
- Cao Jinshan, Wang Guoliang, Liu Jiandong, et al. 2023. Determination of Early Devonian A-type granites in the eastern segment of East Kunlun—Evidences from zircon U-Pb geochronology and elemental geochemistry of dumanyahe biotite granite in east of Wulan area [J]. *Xinjiang Geology*, 41(2): 167~177 (in Chinese with English abstract).
- Chen Haifu, He Shuyue, Zhang Aikui, et al. 2021. Petrogenesis and tectonic setting of Middle Silurian A-type granite in Kaerqueka area, East Kunlun [J]. *Geological Bulletin of China*, 40(8): 1 380~1 393 (in Chinese with English abstract).
- Chen J J, Fu L B, Wei J H, et al. 2020. Proto-Tethys magmatic evolution along northern Gondwana: Insights from late Silurian-middle Devonian A-type magmatism, East Kunlun Orogen, northern Tibetan Plateau, China [J]. *Lithos*, 356: 105304.
- Chen Jianlin, Guo Yuansheng and Fu Shanming. 2004. The research headway to granitoid-classification review and synthesis of isma granitoid [J]. *Acta Geologica Gansu*, 13(1): 67~73 (in Chinese with English abstract).
- Chen N S, Sun M, He L, et al. 2002. Precise timing of the Early Paleozoic metamorphism and thrust deformation in the Eastern Kunlun Orogen [J]. *Chinese Science Bulletin*, 47(13): 1 130~1 133.
- Chen N S, Sun M, Wang Q Y, et al. 2007. EMP chemical ages of monazites from central zone of the eastern Kunlun Orogen: Records of multi-tectonometamorphic events [J]. *Chinese Science Bulletin*, 52(16): 2 252~2 263.
- Creaser R A, Price R C and Wormald R J. 1991. A-type granites revisited: Assessment of a residual-source model [J]. *Geology*, 19(2): 163.
- Ding Q F, Song K, Zhang Q, et al. 2019. Zircon U-Pb geochronology and Hf isotopic constraints on the petrogenesis of the Late Silurian Shidonggou granite from the Wulonggou area in the Eastern Kunlun Orogen, Northwest China [J]. *International Geology Review*, 61(13): 1 666~1 689.
- Dong Y P, He D F, Sun S S, et al. 2018. Subduction and accretionary tectonics of the East Kunlun orogen, western segment of the Central China Orogenic System [J]. *Earth-Science Reviews*, 186: 231~261.
- Dong Y P, Sun S S, Santosh M, et al. 2021. Central China Orogenic Belt and amalgamation of East Asian continents [J]. *Gondwana Research*, 100: 131~194.
- Douce A E P. 1997. Generation of metaluminous A-type granites by low-pressure melting of calc-alkaline granitoids [J]. *Geology*, 25(8): 743~746.
- Duan X P, Meng F C and Jia L H. 2020. Early Paleozoic mantle evolution of East Kunlun Orogenic Belt in Qinghai, NW China: Evidence from the geochemistry and geochronology of the late Ordovician to late Silurian mafic-ultramafic rocks in the qimantag region [J]. *International Geology Review*, 62(15): 1 883~1 903.
- Eby G N. 1992. Chemical subdivision of the A-type granitoids: Petrogenetic and tectonic implications [J]. *Geology*, 20(7): 641.
- Frost C D and Frost B R. 2011. On ferroan (A-type) granitoids: Their compositional variability and modes of origin [J]. *Journal of Petrology*, 52(1): 39~53.
- Fu L B, Bagas L, Wei J H, et al. 2022. Growth of Early Paleozoic continental crust linked to the Proto-Tethys subduction and continental collision in the East Kunlun Orogen, northern Tibetan Plateau [J]. *GSA Bulletin*, 135(7~8): 1 709~1 733.
- Gao Yongbao. 2013. The Intermediate-Acid Intrusive Magmatism and Mineralization in Qimantag, East Kunlun Mountains [D]. Xi'an: Chang'an University, 1~245 (in Chinese with English abstract).
- Guo Xianzheng, Jia Qunzi, Li Jinchao, et al. 2018. Zircon U-Pb geochronology and geochemistry and their geological significances of eclogites from east Kunlun high-pressure metamorphic belt [J]. *Earth Science*, 43(12): 4 300~4 318 (in Chinese with English abstract).
- Hofmann A W, Jochum K P, Seufert M, et al. 1986. Nb and Pb in oce-

- anic basalts: New constraints on mantle evolution [J]. *Earth and Planetary Science Letters*, 79(1~2): 33~45.
- Hu Jichun, Chen Jing, He Shuyue, et al. 2017. Geochronology and petrogenesis of mylonitized granite from Wulonggou area in East Kunlun and its tectonic significance[J]. *Northwestern Geology*, 50(3): 54~64 (in Chinese with English abstract).
- Jia Xiaohui, Wang Qiang and Tang Gongjian. 2009. A-type granites: Research progress and implications[J]. *Geotectonica et Metallogenica*, 33(3): 465~480 (in Chinese with English abstract).
- Jiang Chunfa, Yang Jingsui, Feng Binggui, et al. 1992. Opening-closing Tectonics in Kunlun Mountains[M]. Beijing: Geological Publishing House (in Chinese).
- King P L, White A J R, Chappell B W, et al. 1997. Characterization and origin of aluminous A-type granites from the Lachlan fold belt, southeastern Australia[J]. *Journal of Petrology*, 38(3): 371~391.
- Li C S, Zhang Z W, Li W Y, et al. 2015. Geochronology, petrology and Hf-S isotope geochemistry of the newly-discovered Xialihamu magmatic Ni-Cu sulfide deposit in the Qinghai-Tibet plateau, Western China [J]. *Lithos*, 216: 224~240.
- Li Guochen, Feng Chengyou, Wang Ruijiang, et al. 2012. SIMS zircon U-Pb age, petrochemistry and tectonic implications of granitoids in northeastern baiganhue W-Sn orefield, Xinjiang[J]. *Acta Geoscientifica Sinica*, 33(2): 216~226 (in Chinese with English abstract).
- Li Jiabin, Lü Zeng, Chen Zhenyu, et al. 2023. Metamorphic evolution of mafic two-pyroxene granulites in the Dagele area, East Kunlun[J]. *Acta Petrologica Sinica*, 39(9): 2 636~2 650 (in Chinese with English abstract).
- Li Jiliang, Sun Shu, Hao Jie, et al. 1999. Time limit of collision event of collision orogens [J]. *Acta Petrologica Sinica*, 15(2): 156~161 (in Chinese).
- Li Xi. 2014. Granite Characteristics and Tectonic Setting in Wulonggou Area, East Kunlun[D]. Beijing: China University of Geosciences (Beijing), 1~69 (in Chinese with English abstract).
- Li Xianhua, Liu Xiaoming, Liu Yongsheng, et al. 2015. Accuracy of LA-ICPMS zircon U-Pb age determination: An inter-laboratory comparison[J]. *Science China: Earth Sciences*, 45(9): 1 294~1 303 (in Chinese with English abstract).
- Liu Bin, Ma Changqian, Guo Pan, et al. 2013. Discovery of the middle Devonian A-type granite from the eastern Kunlun Orogen and its tectonic implications[J]. *Earth Science*, 38(5): 947~962 (in Chinese with English abstract).
- Loiselle M C and Wones D R. 1979. Characteristics and origin of anorogenic granites[J]. *Geological Society of America, Abstractm* 11: 468.
- Long L E, Sial A N, Nekvasil H, et al. 1986. Origin of granite at Cabo de santo agostinho, northeast Brazil[J]. *Contributions to Mineralogy and Petrology*, 92(3): 341~350.
- Lu Lu, Wu Zhenhan, Hu Daogong, et al. 2010. Zircon U-Pb age for rhyolite of the Maoniushan Formation and its tectonic significance in the East Kunlun Mountains[J]. *Acta Petrologica Sinica*, 26(4): 1 150~1 158 (in Chinese with English abstract).
- Lu Lu, Zhang Yanlin, Wu Zhenhan, et al. 2013. Zircon U-Pb dating of Early Paleozoic granites from the East Kunlun Mountains and its geological significance[J]. *Acta Geoscientica Sinica*, 34(4): 447~454 (in Chinese with English abstract).
- Lu Songnian, Yu Haifeng, Li Huaikun, et al. 2006. Early Paleozoic suturing zones and tectonic divisions in the “Central China Orogen”[J]. *Geological Bulletin of China*, 25(12): 1 368~1 380 (in Chinese).
- Ma Hongwen. 1992. Discrimination of genetic types of granitoid rocks [J]. *Acta Petrologica Sinica*, 8(4): 341~350 (in Chinese with English abstract).
- Middlemost E A K. 1985. *Magmas and Magmatic Rocks*[M]. London: Longman.
- Middlemost E A K. 1994. Naming materials in the magma/igneous rock system[J]. *Earth-Science Reviews*, 37(3~4): 215~224.
- Miller C F, McDowell S M and Mapes R W. 2003. Hot and cold granites? Implications of zircon saturation temperatures and preservation of inheritance[J]. *Geology*, 31(6): 529~532.
- Pearce J. 1996. Sources and settings of granitic rocks[J]. *Episodes*, 19(4): 120~125.
- Peccerillo A and Taylor S R. 1976. Geochemistry of Eocene calc-alkaline volcanic rocks from the Kastamonu area, northern Turkey[J]. *Contributions to Mineralogy and Petrology*, 58(1): 63~81.
- Pei Xianzhi, Li Ruobao, Li Zuochen, et al. 2018. Composition feature and formation process of buqingshan composite accretionary mélange belt in southern margin of East Kunlun Orogen[J]. *Earth Science*, 43(12): 4 498~4 520 (in Chinese with English abstract).
- Rapp R P and Watson E B. 1995. Dehydration melting of metabasalt at 8~32 kbar: Implications for continental growth and crust-mantle recycling[J]. *Journal of Petrology*, 36(4): 891~931.
- Sun S S and McDonough W F. 1989. Chemical and isotopic systematics of oceanic basalts: Implications for mantle composition and processes [J]. *Geological Society of London Special Publications*, 42(1): 313~345.
- Turner S P, Foden J D and Morrison R S. 1992. Derivation of some A-type magmas by fractionation of basaltic magma: An example from the

- padthaway ridge, South Australia[J]. *Lithos*, 28(2): 151~179.
- Wang Bingzhang, Pan Tong, Ren Haidong, et al. 2021. Cambrian qimantagh island arc in the East Kunlun Orogen: Evidences from zircon U-Pb ages, lithogeochemistry and Hf isotopes of high-Mg andesite/diorite from the lalinggaolihe area [J]. *Earth Science Frontiers*, 28(1): 318~333 (in Chinese with English abstract).
- Wang Guan, Sun Fengyue, Li Bile, et al. 2013. Zircon U-Pb geochronology and geochemistry of the Early Devonian syenogranite in the Xiraihamu ore district from East Kunlun, with implications for the geo-dynamic setting[J]. *Geotectonica et Metallogenesis*, 37(4): 685~697 (in Chinese with English abstract).
- Wang Guocan, Wei Qirong, Jia Chunxing, et al. 2007. Some ideas of Precambrian geology in the East Kunlun, China[J]. *Geological Bulletin of China*, 26(8): 929~937 (in Chinese with English abstract).
- Wang Qiang, Zhao Zhenhua and Xiong Xiaolin. 2000. The ascertainment of late-yanshanian A-type granite in Tongbai-dabie Orogenic Belt[J]. *Acta Petrologica et Mineralogica*, 19(4): 297~306, 315 (in Chinese with English abstract).
- Wang Q L, Zhang J Y, Pan L, et al. 2024. Geochronological and sulfide geochemical evidence for gold mineralization related to post-collisional magmatism in the Wulonggou goldfield of the East Kunlun Orogen, northern Tibet[J]. *Ore Geology Reviews*, 170: 106155.
- Wang Shuai, Li Yingjie, Kong Xingrui, et al. 2022. Ocean basin closure and post orogenic extension in the eastern paleo-Asian ocean: Evidence from Middle Triassic A-type granite in sonid Youqi, Inner Mongolia[J]. *Acta Petrologica et Mineralogica*, 41(3): 555~568 (in Chinese with English abstract).
- Wang Tao, Li Bin, Chen Jing, et al. 2016. Characteristics of chronology and geochemistry of the early Silurian monzogranite in the wulonggou area, east Kunlun and its geological significance[J]. *Journal of Mineralogy and Petrology*, 36(2): 62~70 (in Chinese with English abstract).
- Wang Tong. 2015. Study of the Geological Characteristics and genesis of Wulonggou gold deposit, Qinghai Province[D]. Beijing: China University of Geosciences (in Chinese with English abstract).
- Wang Xiaoxia, Hu Nenggao, Wang Tao, et al. 2012. Late Ordovician wanbaogou granitoid pluton from the southern margin of the Qaidam Basin: Zircon SHRIMP U-Pb age, Hf isotope and geochemistry[J]. *Acta Petrologica Sinica*, 28(9): 2 950~2 962 (in Chinese with English abstract).
- Wang Yilong, Li Yanjun, Wei Junhao, et al. 2018. Origin of late Silurian A-type granite in wulonggou area, East Kunlun Orogen: Zircon U-Pb age, geochemistry, Nd and Hf isotopic constraints[J]. *Earth Science*, 43(4): 1 219~1 236 (in Chinese with English abstract).
- Watson E B and Harrison T M. 1983. Zircon saturation revisited: Temperature and composition effects in a variety of crustal magma types [J]. *Earth and Planetary Science Letters*, 64(2): 295~304.
- Whalen J B, Currie K L and Chappell B W. 1987. A-type granites: Geochemical characteristics, discrimination and petrogenesis[J]. *Contributions to Mineralogy and Petrology*, 95(4): 407~419.
- Wu Fuyuan, Li Xianhua, Yang Jinhui, et al. 2007. Discussions on the petrogenesis of granites[J]. *Acta Petrologica Sinica*, 23(6): 1 217~1 238 (in Chinese with English abstract).
- Wu F Y, Liu X C, Ji W Q, et al. 2017. Highly fractionated granites: Recognition and research[J]. *Science China (Earth Sciences)*, 60(7): 1 201~1 219.
- Wu Suoping, Wang Meiyang and Qi Kaijing. 2007. Present situation of researches on A-type granites: A review[J]. *Acta Petrologica et Mineralogica*, 26(1): 57~66 (in Chinese with English abstract).
- Wu Yuanbao and Zheng Yongfei. 2004. Genetic of zircon and its constraints on interpretation of U-Pb age [J]. *Chinese Science Bulletin*, 49(16): 1 589~1 604 (in Chinese).
- Xin W, Sun F Y, Li L, et al. 2018. The wulonggou metaluminous A2-type granites in the eastern Kunlun Orogenic Belt, NW China: Rejuvenation of subduction-related felsic crust and implications for post-collision extension[J]. *Lithos*, 312: 108~127.
- Xu Zhiqin, Yang Jingsui, Li Haibing, et al. 2006. The Early Palaeozoic terrane framework and the formation of the high-pressure (HP) and ultra-high pressure (UHP) metamorphic belts at the central orogenic belt (COB)[J]. *Acta Geologica Sinica*, 80(12): 1 793~1 806 (in Chinese with English abstract).
- Yan J M, Sun G S, Sun F Y, et al. 2019. Geochronology, geochemistry, and Hf isotopic compositions of monzogranites and mafic-ultramafic complexes in the Maxingdawannan area, eastern Kunlun Orogen, Western China: Implications for magma sources, geodynamic setting, and petrogenesis[J]. *Journal of Earth Science*, 30(2): 335~347.
- Yan Wei, Qiu Dianming, Ding Qingfeng, et al. 2016. Geochronology, petrogenesis, source and its structural significance of Houtougou monzogranite of Wulonggou area in eastern Kunlun Orogen[J]. *Journal of Jilin University (Earth Science Edition)*, 46(2): 443~460 (in Chinese with English abstract).
- Yang J H, Wu F Y, Chung S L, et al. 2006. A hybrid origin for the Qianshan A-type granite, Northeast China: Geochemical and Sr-Nd-Hf isotopic evidence[J]. *Lithos*, 89(1~2): 89~106.
- Yu M, Feng C Y, Santosh M, et al. 2017. The Qiman Tagh Orogen as a

- window to the crustal evolution in northern Qinghai-Tibet Plateau[J]. Earth-Science Reviews, 167: 103~123.
- Zhang J Y, Lei H L, Ma C Q, et al. 2021. Silurian-Devonian granites and associated intermediate-mafic rocks along the eastern Kunlun Orogen, Western China: Evidence for a prolonged post-collisional lithospheric extension[J]. Gondwana Research, 89: 131~146.
- Zhang Liang, Li Bile, Liu Lei, et al. 2021. Geochronology, geochemistry and geological significance of the Early Devonian bimodal intrusive rocks in Wulonggou area, East Kunlun Orogen[J]. Acta Petrologica Sinica, 37(7): 2 007~2 028 (in Chinese with English abstract).
- Zhang Qi, Ran Hao and Li Chengdong. 2012. A-type granite: What is the essence? [J]. Acta Petrologica et Mineralogica, 31(4): 621~626 (in Chinese with English abstract).
- Zhao X, Fu L B, Wei J H, et al. 2019. Late Permian back-arc extension of the eastern paleo-Tethys ocean: Evidence from the East Kunlun Orogen, northern Tibetan Plateau[J]. Lithos, 340: 34~48.
- Zheng Z, Chen Y J, Deng X H, et al. 2018. Origin of the Bashierxi monzogranite, Qimantagh, East Kunlun Orogen, NW China: A magmatic response to the evolution of the Proto-Tethys Ocean [J]. Lithos, 296: 181~194.
- Zhou J H, Feng C Y, Li D X, et al. 2016. Geological, geochemical, and geochronological characteristics of Caledonian W-Sn mineralization in the Baiganhu orefield, southeastern Xinjiang, China[J]. Ore Geology Reviews, 75: 125~149.
- 陈能松,孙敏,王勤燕,等. 2007. 东昆仑造山带昆中带的独居石电子探针化学年龄:多期构造变质事件记录[J]. 科学通报, 52(11): 1 297~1 306.
- 高永宝. 2013. 东昆仑祁漫塔格地区中酸性侵入岩浆活动与成矿作用[D]. 西安: 长安大学, 1~245.
- 国显正,贾群子,李金超,等. 2018. 东昆仑高压变质带榴辉岩年代学、地球化学及其地质意义[J]. 地球科学, 43(12): 4 300~4 318.
- 胡继春,陈静,何书跃,等. 2017. 东昆仑五龙沟地区糜棱岩化花岗岩年代学、岩石成因及其构造意义[J]. 西北地质, 50(3): 54~64.
- 贾小辉,王强,唐功建. 2009. A型花岗岩的研究进展及意义[J]. 大地构造与成矿学, 33(3): 465~480.
- 姜春发,杨经绥,冯秉贵,等. 1992. 昆仑开合构造[M]. 北京: 地质出版社.
- 李国臣,丰成友,王瑞江,等. 2012. 新疆白干湖钨锡矿田东北部花岗岩锆石SMS U-Pb年龄、地球化学特征及构造意义[J]. 地球学报, 33(2): 216~226..
- 李继亮,孙枢,郝杰,等. 1999. 碰撞造山带的碰撞事件时限的确定[J]. 岩石学报, 15(2): 156~161.
- 李佳斌,吕增,陈振宇,等. 2023. 东昆仑大格勒一带基性二辉麻粒岩的变质演化及地质意义[J]. 岩石学报, 39(9): 2 636~2 650.
- 李希. 2014. 东昆仑五龙沟地区花岗岩特征与构造背景[D]. 北京: 中国地质大学(北京), 1~69.
- 李献华,柳小明,刘勇胜,等. 2015. LA-ICPMS锆石U-Pb定年的准确度: 多实验室对比分析[J]. 中国科学: 地球科学, 45(9): 1 294~1 303.
- 刘彬,马昌前,郭盼,等. 2013. 东昆仑中泥盆世A型花岗岩的确定及其构造意义[J]. 地球科学, 38(5): 947~962.
- 陆露,吴珍汉,胡道功,等. 2010. 东昆仑牦牛山组流纹岩锆石U-Pb年龄及构造意义[J]. 岩石学报, 26(4): 1 150~1 158.
- 陆露,张延林,吴珍汉,等. 2013. 东昆仑早古生代花岗岩锆石U-Pb年龄及其他地质意义[J]. 地球学报, 34(4): 447~454.
- 陆松年,于海峰,李怀坤,等. 2006. “中央造山带”早古生代缝合带及构造分区概述[J]. 地质通报, 25(12): 1 368~1 380.
- 马鸿文. 1992. 花岗岩成因类型的判别分析[J]. 岩石学报, 8(4): 341~350.
- 裴先治,李瑞保,李佐臣,等. 2018. 东昆仑南缘布青山复合增生型构造混杂岩带组成特征及其形成演化过程[J]. 地球科学, 43(12): 4 498~4 520.
- 王秉璋,潘彤,任海东,等. 2021. 东昆仑祁漫塔格寒武纪岛弧: 来自拉陵高里河地区玻安岩型高镁安山岩/闪长岩锆石U-Pb年

附中文参考文献

- 包长甲,柴凤梅,李永,等. 2021. 新疆阿尔泰巴斯铁列克钨多金属矿区花岗岩体年代学和地球化学特征及其对成矿的启示[J]. 岩石学报, 37(3): 886~910.
- 曹锦山,王国良,刘建栋,等. 2023. 东昆仑东段早泥盆世“A”型花岗岩的确定——来自乌兰东地区都南哑合黑云母花岗岩锆石U-Pb年代学、元素地球化学证据[J]. 新疆地质, 41(2): 167~177.
- 陈海福,何书跃,张爱奎,等. 2021. 东昆仑卡尔却卡地区中志留世A型花岗岩岩石成因及构造环境[J]. 地质通报, 40(8): 1 380~1 393.
- 陈建林,郭原生,付善明. 2004. 花岗岩研究进展——ISMA花岗岩类分类综述[J]. 甘肃地质学报, 13(1): 67~73.
- 陈能松,孙敏,何蕾,等. 2002. 东昆仑造山带早古生代变质高峰期和逆冲构造变形年代的精确限定[J]. 科学通报, 47(8): 628~631.

- 代学、地球化学和 Hf 同位素证据 [J]. 地学前缘, 28(1): 318~333.
- 王冠, 孙丰月, 李碧乐, 等. 2013. 东昆仑夏日哈木矿区早泥盆世正长花岗岩锆石 U-Pb 年代学、地球化学及其动力学意义 [J]. 大地构造与成矿学, 37(4): 685~697.
- 王国灿, 魏启荣, 贾春兴, 等. 2007. 关于东昆仑地区前寒武纪地质的几点认识 [J]. 地质通报, 26(8): 929~937.
- 王强, 赵振华, 熊小林. 2000. 桐柏一大别造山带燕山晚期 A 型花岗岩的厘定 [J]. 岩石矿物学杂志, 19(4): 297~306, 315.
- 王帅, 李英杰, 孔星蕊, 等. 2022. 古亚洲洋东段洋盆闭合与后造山伸展——来自内蒙古苏尼特右旗中三叠世 A 型花岗岩的证据 [J]. 岩石矿物学杂志, 41(3): 555~568.
- 王涛, 李彬, 陈静, 等. 2016. 东昆仑五龙沟地区早志留世花岗岩锆石年代学、地球化学特征及其地质意义 [J]. 矿物岩石, 36(2): 62~70.
- 王铜. 2015 青海五龙沟金矿床地质特征与成因研究 [D]. 北京: 中国地质大学(北京).
- 王晓霞, 胡能高, 王涛, 等. 2012. 柴达木盆地南缘晚奥陶世万宝沟花岗岩: 锆石 SHRIMP U-Pb 年龄、Hf 同位素和元素地球化学 [J]. 岩石学报, 28(9): 2 950~2 962.
- 王艺龙, 李艳军, 魏俊浩, 等. 2018. 东昆仑五龙沟地区晚志留世 A 型花岗岩成因: U-Pb 年代学、地球化学、Nd 及 Hf 同位素制约 [J]. 地球科学, 43(4): 1 219~1 236.
- 吴福元, 李献华, 杨进辉, 等. 2007. 花岗岩成因研究的若干问题 [J]. 岩石学报, 23(6): 1 217~1 238.
- 吴福元, 刘小驰, 纪伟强, 等. 2017. 高分异花岗岩的识别与研究 [J]. 中国科学: 地球科学, 47(7): 745~765.
- 吴锁平, 王梅英, 戚开静. 2007. A 型花岗岩研究现状及其述评 [J]. 岩石矿物学杂志, 26(1): 57~66.
- 吴元保, 郑永飞. 2004. 锆石成因矿物学研究及其对 U-Pb 年龄解释的制约 [J]. 科学通报, 49(16): 1 589~1 604.
- 许志琴, 杨经绥, 李海兵, 等. 2006. 中央造山带早古生代地体构架与高压/超高压变质带的形成 [J]. 地质学报, 80(12): 1 793~1 806.
- 严威, 邱殿明, 丁清峰, 等. 2016. 东昆仑五龙沟地区猴头沟二长花岗岩年龄、成因、源区及其构造意义 [J]. 吉林大学学报(地球科学版), 46(2): 443~460.
- 张亮, 李碧乐, 刘磊, 等. 2021. 东昆仑五龙沟地区早泥盆世双峰式侵入岩年代学、地球化学及其地质意义 [J]. 岩石学报, 37(7): 2 007~2 028.
- 张旗, 冉皞, 李承东. 2012. A 型花岗岩的实质是什么? [J]. 岩石矿物学杂志, 31(4): 621~626.